LA-UR- 09-04139

Approved for public release; distribution is unlimited.

Title:	Detection Limits for Actinides in a Monochromatic, Wavelength-Dispersive X-Ray Fluorescence Instrument
Author(s):	Michael L. Collins, LANL Group N-4 George J. Havrilla, LANL Group C-CDE
Intended for:	Institute of Nuclear Materials Management 50th Annual Meeting July 12-16, 2009 JW Marriott Starr Pass Tucson, Arizona, USA

Los Alamos
NATIONAL LABORATORY
EST. 1943

Form 836 (7/06)

Detection Limits for Actinides in a Monochromatic, Wavelength-Dispersive X-Ray Fluorescence Instrument

Michael L. Collins, LANL Group N-4

George Havrilla, LANL Group C-AAC

ABSTRACT

Recent developments in x-ray optics have made it possible to examine the L x-rays of actinides using doubly-curved crystals in a bench-top device. A doubly-curved crystal (DCC) acts as a focusing monochromatic filter for polychromatic x-rays. A Monochromatic, Wavelength-Dispersive X-Ray Fluorescence (MWDXRF) instrument that uses DCCs to measure Cm and Pu in reprocessing plant liquors was proposed in 2007 by the authors at Los Alamos National Laboratory. A prototype design of this MWDXRF instrument was developed in collaboration with X-ray Optical Systems Inc. (XOS), of East Greenbush, New York. In the MWDXRF instrument, x-rays from a Rhodium-anode x-ray tube are passed through a primary DCC to produce a monochromatic beam of 20.2-keV photons. This beam is focused on a specimen that may contain actinides. The 20.2-keV interrogating beam is just above the L3 edge of Californium; each actinide (with Z=90 to 98) present in the specimen emits characteristic L x-rays as the result of L3-shell vacancies. In the LANL-XOS prototype MWDXRF, these x-rays enter a secondary DCC optic that preferentially passes 14.961-keV photons, corresponding to the L-alpha-1 x-ray peak of Curium. In the present stage of experimentation, Curium-bearing specimens have not been analyzed with the prototype MWDXRF instrument. Surrogate materials for Curium include Rubidium, which has a K-beta-1 x-ray at 14.961 keV, and Yttrium, which has a K-alpha-1 x-ray at 14.958 keV.

In this paper, the lower limit of detection for Curium in the LANL-XOS prototype MWDXRF instrument is estimated. The basis for this estimate is described, including a description of computational models and benchmarking techniques used. Detection limits for other actinides are considered, as well as future safeguards applications for MWDXRF instrumentation.

DESCRIPTION OF INSTRUMENT

In May 2009, experiments were performed using a "breadboard" (earliest prototype) MWDXRF system at the headquarters of X-ray Optical Systems (XOS), Inc. in East Greenbush, New York. The breadboard system consisted of five main components: a microfocus x-ray generator, an "excitation" doubly-curved crystal (DCC) x-ray optic, a sample holder, a "collection" DCC x-ray optic, and a silicon-pin diode detector. Additionally, a video camera with zoom lens was used for visual guidance in the positioning of samples. The breadboard system is illustrated in Figure 1 .

The microfocus x-ray generator was an XOS X-Beam model with a Rhodium anode. The x-ray generator had a maximum tube voltage of 50 kiloVolts and maximum tube current of one Ampere. The maximum power of the x-ray tube was therefore 50 Watts; the tube was air-cooled. The Rhodium anode of the x-ray

tube, when bombarded with 50 keV electrons, emits the characteristic x-ray lines of Rhodium superimposed on a *bremsstrahlung* background. The most prominent x-ray emitted from the anode is the Rhodium Ka1 peak, which has a centroid of 20.21 keV. Rhodium (Z=45) was selected as the anode material because the Rh Ka1 peak lies above the L3 edge of Curium (18.97 keV). Ideally we would interrogate with a photon beam whose energy is just above the Cm L3 edge, but Ruthenium (Z=44, with Ka1 peak at 19.28 keV) was not a practical choice for this experiment. Rhodium Ka1 x-rays produced in the x-ray tube have a Lorentzian energy distribution, centered at 20.21 keV, with a line width (full width at half-maximum) of 9.77 eV.

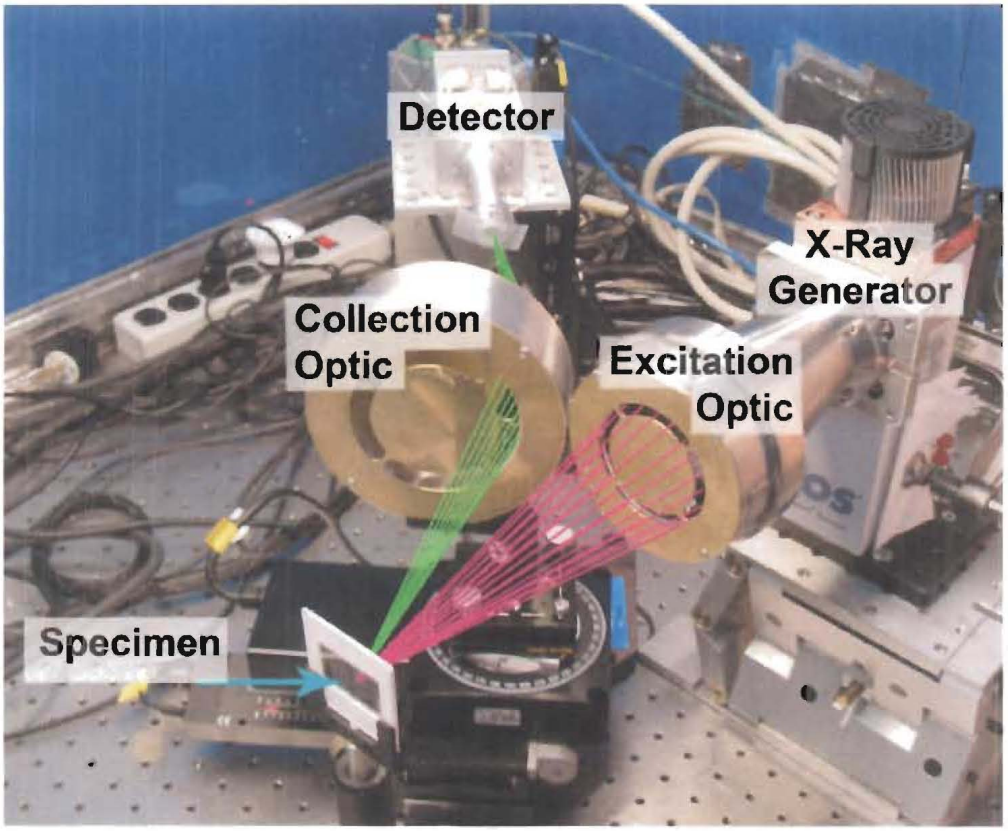

Figure 1. Breadboard MWDXRF system for detection of Curium La1 x-rays. *The X-Ray Generator produces a polychromatic beam of Rhodium x-rays and bremsstrahlung photons. Some radiation from the tube enters the Excitation Optic, which selectively passes 20.2 keV (Rh Ka1) photons and directs them toward the Specimen. Scattered photons and fluoresced x-rays are emitted from the specimen (and substrate) in all directions. Some radiation from the specimen enters the Collection Optic aperture. The collection optic selectively passes 14.96 keV (Cm La1, Y Ka1, Rb Kb1) photons and directs them toward the Detector. Green and magenta line segments were added for illustration purposes.*

The Excitation Optic was a Doubly-Curved Crystal optimized for 20.2 keV photons. This optic was manufactured by XOS Inc., with a point-to-point focal length of 400 mm. This optic contained four 90-degree segments, which together formed a toroidal Bragg scattering surface for x-rays. Paths of photons leaving the excitation optic are illustrated with magenta line segments in Figure 1.

The specimen consists of a dried spot of nitric acid solution, deposited on a 4 um thick polypropylene film substrate. The substrate was held in a type 135 slide frame (5 cm by 5 cm, the size of a "35 mm" photographic slide). The slide frame was mounted on a motorized three-dimensional (X, Y, Z) translation stage. A video camera with telescopic lens was trained on the focal spot of the x-ray beam to assist with source positioning.

The Collection Optic was a Doubly-Curved Crystal optimized for 14.96 keV photons. This optic was custom manufactured for this experiment by XOS Inc., with a point-to-point focal length of 400 mm. This optic contained one 90-degree segment, which subtended one-quarter revolution of azimuth around the specimen-to-detector axis. Paths of photons entering the collection optic and scattered toward the detector are illustrated with green line segments in Figure 1.

FORMATION OF DRIED DEPOSITS

A one-microliter droplet of aqueous solution (as featured in this paper, 10 ug/ml Yttrium) was deposited onto 4 um thick polypropylene film and allowed to dry. While evaporating, the droplet does not maintain its original footprint, nor are the contents of the droplet deposited evenly amongst the original contact area.

One microliter has the same volume as a cubic millimeter. A one-microliter droplet is approximately spherical, with a diameter of about 1.24 mm, prior to deposition on the film. When the droplet contacts the film, the droplet assumes a truncated spherical shape. The upper hemisphere is complete, but the lower hemisphere is truncated below the film/droplet interface. The film/droplet interface (footprint) is nominally circular in shape. The diameter of the film/droplet interface is the "contact diameter", and the area of this interface is the "contact area". As the droplet evaporates, the contact diameter shrinks dramatically.

A Japanese study of microliter-scale water droplets (REF. 3) showed that when deposited on a smooth substrate, the droplet maintains a truncated spherical shape with ever-decreasing contact angle. Figure 2 shows side-view "snapshots" of a microliter-scale water droplet at various times during a 21-minute period.

After evaporation, the 1 microliter droplet with 10 ug/ml Yttrium left a dried deposit approximately 400 um in diameter. This observation suggests that the contact area of the wet Yttrium-bearing droplet shrinks significantly before any appreciable dried deposit forms on the substrate. The Furuta data suggests that the volume of our Yttrium solution decreases by a factor of 100 or more before a discernable outer ring of dry deposit begins to form. Perhaps formation of the outer ring (and precipitation of solids) begins when the concentration of solutes in the droplet exceeds a certain value.

With the MWDXRF instrument, it is advantageous for the dried deposit to be only slightly smaller than the diameter of the excitation beam. This would help to maximize signal response, because the full dried deposit would be exposed to x-ray interrogation.

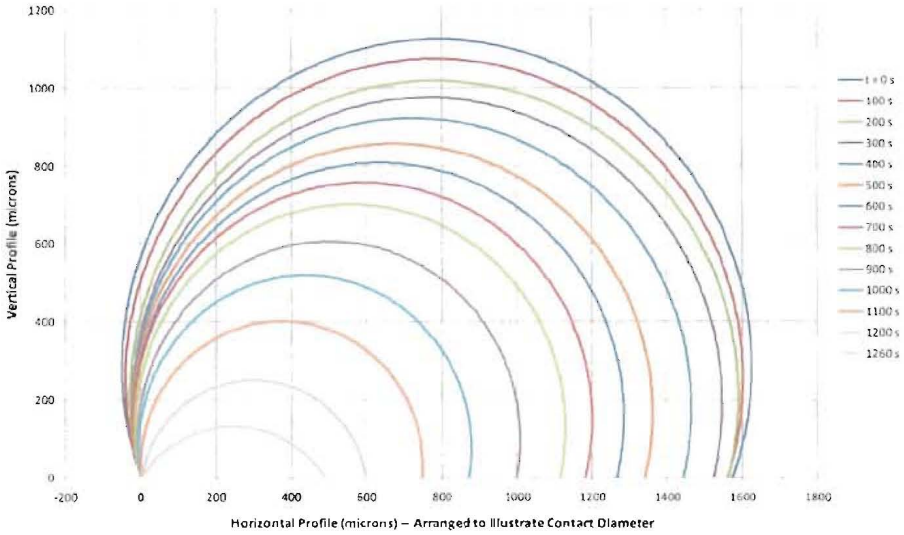

Figure 2. Side profile of microliter-scale water droplet during evaporation. *Deduced by author from contact angle and contact radius data in Furuta et. al. 2009. At time zero, the droplet is a truncated sphere with contact diameter 1570 um and height 1120 um. After 21 minutes, the droplet has lost 99 percent of its volume, and the contact area has shrunk by 90 percent.*

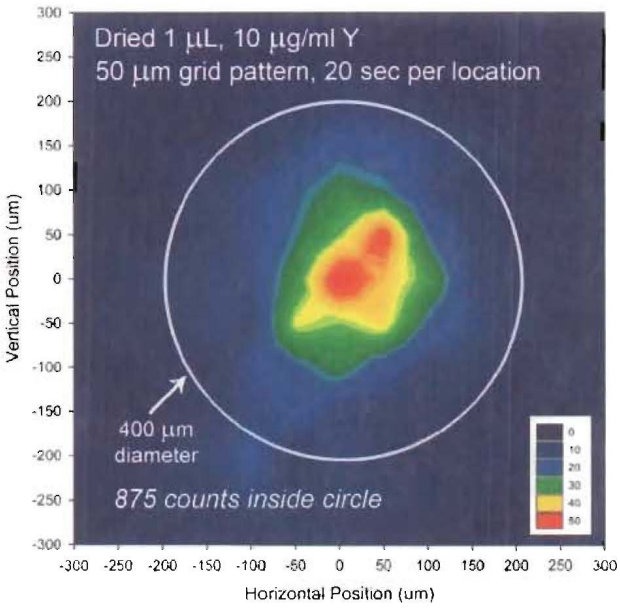

Figure 3. Map of Dried Deposit for 10 ug/mL Yttrium. *Original wet droplet volume 1 uL.*

When only a single dried deposit is being analyzed, there is no incentive for the deposit to be much smaller than the beam. Suppose we start with a dried deposit that is exactly the same diameter as the beam, and consider two cases. In case 1, we keep the mass of the deposit the same, but shrink the area. The deposit would necessarily be thicker, causing a slight loss of signal due to increased self-attenuation

of 14.9 keV x-rays. In case 2, we keep the areal density of the deposit the same, but shrink the area. In that case there is a loss of signal due to decreased mass of the deposit.

In the case of the 1 microliter droplet with 10 ug/ml Yttrium, the dried deposit (400 um diameter) was about 4 times the area of the beam spot (200 um diameter). If areal mass density and composition were uniform throughout the deposit, we could point the beam anywhere at the deposit and get the same count rate in the 14.96 keV region of interest. In reality the areal mass density of Yttrium varied throughout the deposit, as evidenced by a two-dimensional map of deposit. The map in Figure 3 was obtained by displacing the specimen vertically and horizontally in an automatic sequence of measurements. The grid pattern had a spacing of 50 micrometers in the X and Y directions. Each location in the grid pattern was measured for 20 seconds, at which the number of counts in the region of interest for the 14.9 keV peak was recorded. The maximum number of counts was 54 at the origin. The sum of all counts for grid points located 200 um or less from the origin was 875.

To better understand the distribution of Yttrium in the dried deposit, it is helpful to examine data from the Figure 3 another way. Figure 4 shows the same data from Figure 3, but in this case the number of counts observed at each grid point is plotted versus distance of the grid point from the origin.

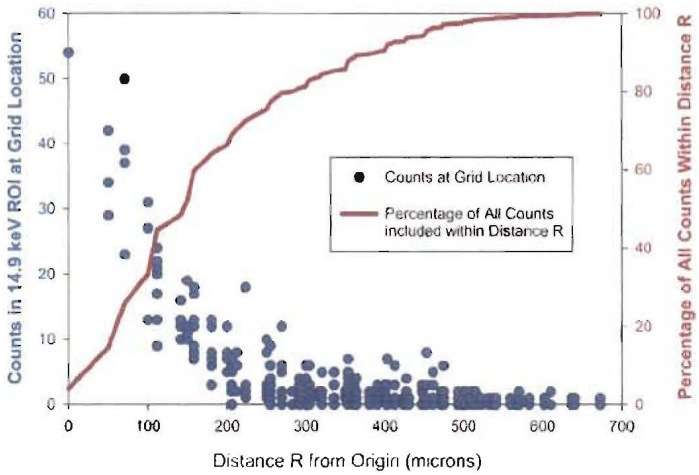

Figure 4. Radial distribution of counts from dried deposit map. *Deposit was initially a 1 uL droplet of 10 ug/ml Yttrium solution. Blue dots (scale on left vertical axis) indicate radial distribution of counts in 14.9 keV region of interest. Red line (scale on right vertical axis) indicates cumulative percentage of all counts that lie within distance R from origin. Approximately two-thirds of the total observed counts were within 200 um of the origin. The count time at each grid location was 20 seconds.*

The radial distribution of counts in Figure 4 shows that the areal density of dried Yttrium deposits far from the origin is very low. The mapping exercise covered a 20-row by 20-column grid, with rows and columns spaced 50 microns apart. Therefore the map consists of 400 grid points on a 1mm-by-1mm square; only a portion of the mapped area was shown in Figure 3. This grid mapping exercise required 8000 seconds of live time (about 2 hours 14 minutes). It would not be practical to measure every specimen with a large grid pattern. However, a 1 microliter droplet produces a dried deposit that is several times the area of the beam spot. If absolute concentration of the analyte is desired (ug/ml) for microliter-scale samples, a grid-pattern measurement would be the preferred approach.

The 200-micron radius circle (area 0.125 mm2) at center contains 66% of the observed counts, and has an average areal mass density of 53 ngY/mm2. The annular ring from radius 200 um to 400 um has an area of 0.38 mm2, and average areal mass density of 6.4 ngY/mm2. The annular ring from radius 400 um to 600 um has an area of 0.63 mm2, and average areal mass density of 1.4 ngY/mm2.

This radial distribution of Yttrium suggests that a smaller droplet footprint (contact diameter) at the time of deposition would allow a smaller grid pattern to be used. Pre-concentration (evaporation) of the wet solution prior to deposition would result in dried spots that have a sharper boundary. Pre-concentration of the 10 ug/ml Yttrium solution by a factor of 10 would shrink the initial droplet volume by a factor of 10, and would shrink the initial contact area by a factor of four.

BASIS MEASUREMENT

To calculate a limit of detection for Yttrium, we observe the response in our detector for a known quantity of analyte. We measured the number of counts in a predefined region of interest for the 14.96 keV Ka1 x-ray of Yttrium. The specimen in our basis measurement was the 10 ug/ml dried deposit as featured in the previous section. In this case the beam spot was centered at the origin of Figure 3 above. The region of interest in the multichannel analyzer included 21 channels of data, ranging in energy from 14.48 keV to 15.45 keV. The specimen was measured for 100 seconds. A blank sample (dried water on polypropylene film) was measured separately for 1000 seconds. The observed spectra are shown in Figure 5.

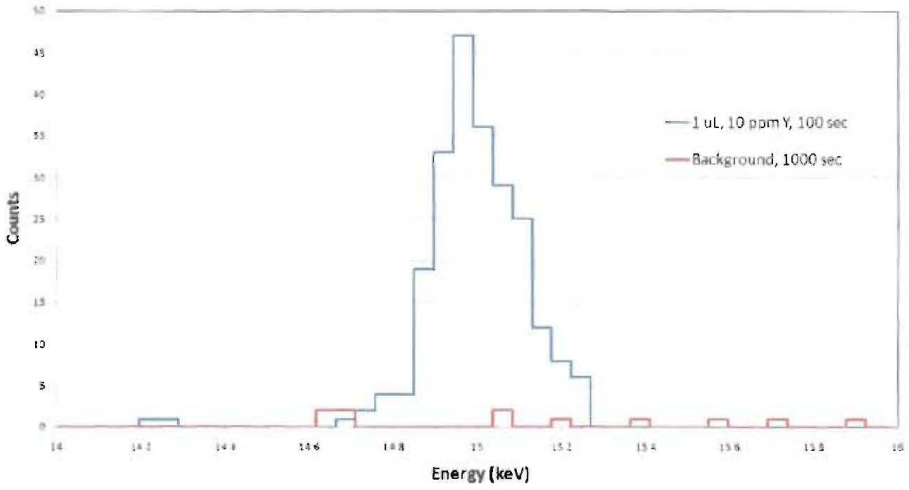

Figure 5. Observed spectra (specimen and background)

In the spectrum for the specimen, 226 counts were observed in the 14.9 keV region of interest during a 100-livetime-second acquisition. The basis count rate was 2.26 counts per second. In the background spectrum, a total of 8 counts were observed in the ROI during a 1000-second acquisition. The background count rate was 0.008 counts per second.

Poisson statistics dictate that when 226 counts are observed in 100 seconds, we can say with 95 percent confidence that the nominal count rate for the specimen was between 1.99 and 2.57 counts per second. Similarly, when 8 background counts are observed in 1000 seconds, we can say with 95 percent

confidence that the nominal background rate was between 0.004 and 0.016 counts per second. To err on the side of caution, consider a "worst case scenario" with lowest signal and highest background. In that scenario, the observed rate with specimen is 1.99 counts per second, and the observed background rate is 0.016 counts per second. During a 100 second count, this would correspond to a specimen tally of 199 counts, and a background tally of 2 counts. The net signal is 197 counts, with an absolute uncertainty of 14 counts. The uncertainty in the net signal rate is 9 times higher than the background rate itself.

LIMIT OF DETECTION FOR YTTRIUM

Detection limits in this paper are derived from methods and techniques described by Gedcke (REF. 8) in the section "Detection Limits With Zero Background". It is necessary to define a threshold for the number of counts acquired in the 14.9 keV region of interest during a single measurement. If the observed number of counts exceeds the threshold, we can claim detection of the analyte with a prescribed degree of confidence.

The minimum detectable amount of analyte will produce, on average, a number of counts M. The average number of counts M is the mean value that one would obtain by performing a large number of trials; M does not have to be an integer. Using Poisson statistics one can determine the required value of M so that in 95 percent of trials, the observed number of counts X will exceed a predefined threshold T. This defines the "95 percent confidence limit" for detection of the analyte.

$$P_{X>T} = 1 - P_{X\leq T} = 1 - \sum_{j=0}^{T} P_p(j, M) = 0.95 \qquad (1)$$

$$\sum_{j=0}^{T} P_p(j, M) = 0.05 \qquad (2)$$

Values of M that satisfy equation 2 were determined for three different values of threshold T. The first case, T=0 counts, is a true "Zero Background" case in which $M_0 = 2.996$. If there is truly no background, and the average number of counts is 2.996 or higher, and we detect one or more counts, we can be 95 percent certain the analyte has been detected. With a threshold of 1 count, the required average number of counts is $M_1 = 4.744$. With a threshold of 2 counts, the required average number of counts is M2 = 6.296. Poisson distributions for these cases are illustrated in Figure 6 below.

We can now calculate the detection limit for Yttrium. Recall that for a solution of Yttrium with partial density 10 ugY/ml, 226 counts were observed in 100 seconds. If we assume there is zero background, the partial density at the lower limit of detection for a 100 second measurement is:

$$PD_{Y,LLD} = \frac{PD_{Y,Basis}}{S_{Basis}} S_{LLD} = \frac{(10\ \mu gY/ml)}{(226\ cts)} (2.996\ cts) = 0.133\ \mu gY/ml$$

If we instead assume a 1-count background threshold, the lower limit of detection for a 100 second measurement is:

$$PD_{Y,LLD} = \frac{(10\ \mu gY/ml)}{(226\ cts)}(4.744\ cts) = 0.210\ \mu gY/ml$$

In the last case, if a 2-count background threshold were indicated, the lower limit of detection for a 100 second measurement would be:

$$PD_{Y,LLD} = \frac{(10\ \mu gY/ml)}{(226\ cts)}(6.296\ cts) = 0.279\ \mu gY/ml$$

The observed background rate was 0.8 counts per 100 seconds. This suggests that a threshold of 1 count adequately describes the background. Therefore 0.21 µgY/mL is a good estimate of the lower limit of detection for Yttrium (for 100 second count, with dried 1 uL droplet, expressed in terms of partial density).

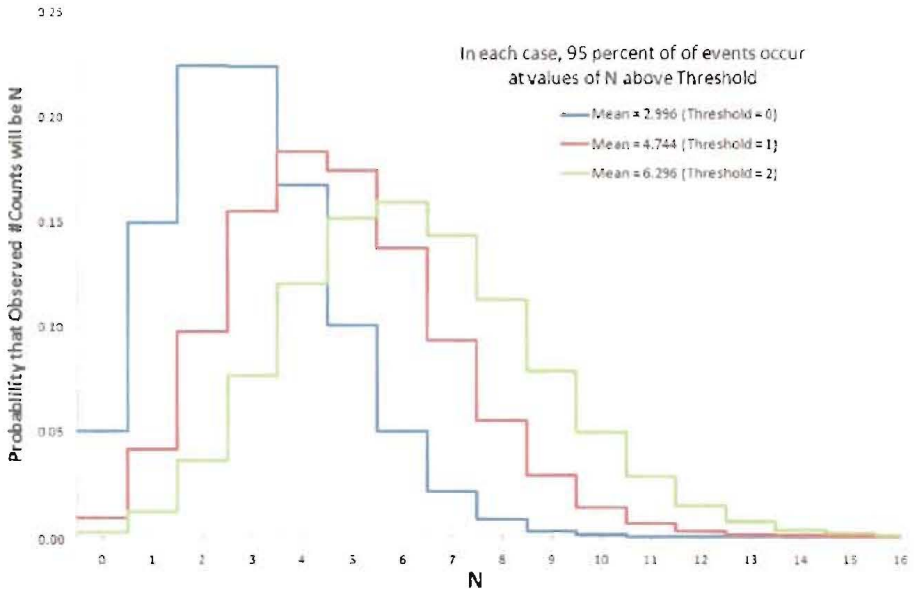

Figure 6. Poisson Distributions for detection of analyte with 95 percent confidence, given background thresholds of 0, 1, and 2 counts. For each profile, 95 percent of trials produce an observed number of counts that exceeds the Threshold.

Another quantity of interest is the mass detection limit for Yttrium. Referring again to Figure 4, approximately 33 percent of all counts in the mapping exercise were attributed to grid points 100 microns from the origin or closer. This suggests that one-third of the Yttrium in the dried deposit (total 10 ng) was within the beam spot when the beam was centered at the origin, such as during the basis measurement.

$$M_{Y,LLD} = \frac{M_{Y,Basis}}{S_{Basis}} S_{LLD} = \frac{(3.3\ ng\ Y)}{(226\ cts)}(4.744\ cts) = 0.069\ ng\ Y = 69\ pg\ Y$$

The estimated lower limit of detection, expressed in terms of Yttrium mass within the beam spot, is 69 picograms during a 100 second measurement. This mass estimate does not depend on wet droplet volume

or partial density of Yttrium in the droplet, and assumes a nearly-uniform areal distribution of Yttrium within the beam spot.

MONTE CARLO SIMULATION

A detailed Monte Carlo N-Particle X (MCNPX) particle transport simulation model of the MWDXRF system was prepared, and several simulated trials were performed. It quickly became obvious that the photoatomic data used by the MCNPX program (in the MCPLIB04 photoatomic data library) did not faithfully emulate real L x-ray fluorescence properties of Curium. An example of unrealistic L XRF simulation results for Curium is shown in Figure 7.

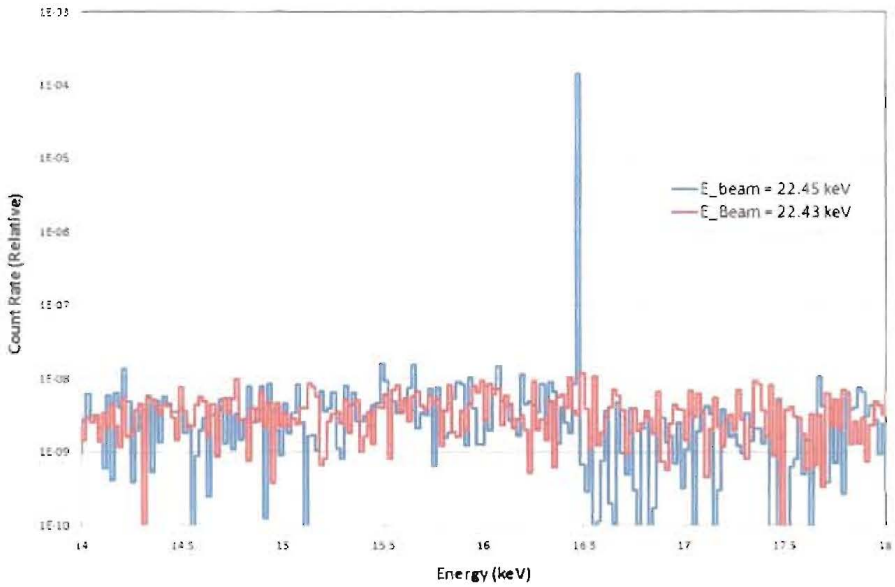

Figure 7. Oversimplified treatment of Curium L-edges and L x-rays in MCNPX. *Spectra from two simulated energy-dispersive XRF measurements of a Curium sample. One spectrum shows results from interrogating with a beam of 22.43 keV photons; no L x-rays are visible. Another spectrum shows the result of interrogating the same with 22.45 keV photons. In that case, a fictitious 16.5 keV x-ray peak appears. Together, these spectra demonstrate a fictitious Cm L edge at 22.44 keV.*

In reality, Curium has 3 L edges (L3 at 18.97 keV, L2 at 23.65 keV, and L1 at 24.53 keV). MCNPX approximates these as a single L edge at 22.44 keV. In reality, Curium has 14 commonly tabulated L x-rays, ranging in energy from 12.63 keV to 23.53 keV. MCNPX approximates these as a single x-ray peak at 16.5 keV. The fictitious 16.5 keV x-ray peak is 0.8 keV away from the nearest tabulated Curium x-ray.

Further study into the treatment of photoatomic data by MCNPX showed that one cannot simply edit a cross section file to add realistic simulation of L x-rays of the actinides. It is possible to relocate the one fictitious L-edge and one fictitious L x-ray, but specifying the correct cross section jump at the edge and correct and x-ray intensity would be tedious. To properly simulate 3 L-edges and numerous L x-rays, modification of the MCNPX program itself would be necessary. Once that obstacle was discovered, MCNPX was abandoned as a prediction tool for this study. A workaround method was devised, involving tabulated x-ray fluorescence cross sections for the elements.

MWDXRF DETECTION LIMITS FOR ACTINIDES

The goal of this paper was to predict MWDXRF detection limits for actinides of safeguards interest. Of these, only Curium, with an La1 x-ray at 14.96 keV, can be measured with the present breadboard system.

Table 1. Predicted Detection Limits for various actinides. *Entries marked with an asterisk (*) would require a new collection optic to be fabricated.*

Z	Analyte ID	X-Ray	X-Ray Energy (keV)	X-Ray Production Cross Section at 20.2 keV (cm^2 g^-1)	Analyte Mass Per Fluoresced X-Ray Relative to Y	Estimated LLD (picograms in beam spot)	Estimated LLD (μg/mL in 1μL droplet)
39	Yttrium	$K_{\alpha 1}$	14.958	22.13	1.00	69	0.21
90	Thorium	$L_{\alpha 1}$	12.968	12.06	1.83	127*	0.39*
92	Uranium	$L_{\alpha 1}$	13.618	12.39	1.79	123*	0.37*
93	Neptunium	$L_{\alpha 1}$	13.946	13.27	1.67	115*	0.35*
94	Plutonium	$L_{\alpha 1}$	14.282	14.04	1.58	109*	0.33*
95	Americium	$L_{\alpha 1}$	14.62	14.81	1.49	103*	0.31*
96	Curium	$L_{\alpha 1}$	14.961	15.48	1.43	99	0.30

The fifth column of Table 1 contains X-ray production cross sections evaluated at 20.2 keV. These cross sections were derived from tabulated data published by Krause et. al. For example, the x-ray production cross section for the Yttrium Ka1 x-ray is 22.13 cm^2 g^-1, and is 15.48 cm^2 g^-1 for the Curium L x-ray.

This tells us that if we had samples of Y and Cm with equal areal mass densities, and interrogated them with an equal intensity of 20.2 keV photons, the Yttrium sample would produce (22.13/15.48) = 1.43 times as many 14.96 keV x-rays as the Curium sample. Conversely, if we interrogated a Y sample and a Cm sample and found that their production rate of 14.96 keV x-rays was equal, we could deduce that the ratio of Curium mass to Yttrium mass is 1.43. To achieve the minimum detectable count rate of 4.744 counts in 100 seconds (and exceed the threshold of one background count with 95 percent confidence), we calculated that 69 picograms of Yttrium were needed. Therefore the required mass of Curium to achieve the same count rate is 1.43*69 = 99 picograms. Similar logic applies to the limits expressed in partial density (ug/mL), as shown in the rightmost column of Table 1.

It is worth noting that when the MWDXRF breadboard system was tested in May 2009, the collection optic was only partially assembled. The collection optic had only one of its four optical elements installed. After all segments of the collection optic are assembled (by the end of FY 2009), the detection limits stated in this paper should drop by nearly a factor of four.

REFERENCES